

# Path Tracking Control of Four Wheel Independently Steered Ground Robotic Vehicles

Majura F. Selekwa and Jonathan R. Nistler

**Abstract**—Because of their high degree of maneuverability, four wheel steered robotic vehicles have increasingly attracted interest in many applications. These robots are characterized by ability to easily maneuver tight turns. Two types of such vehicles have been identified: vehicles with independently steered wheels, and vehicles with mechanically coupled pairs of steered wheels. While the latter group has been easy to model and control, the former group still poses many control challenges. The common approaches employed in modeling and controlling vehicles with independently steered wheels either assume that the rear wheels will copy the front steering angles or allow wheel slippage to accommodate independent steering angles for all wheels. Both these approaches do not offer the sought maneuverability advantages. This paper revisits the problem of four independent wheel steering and proposes an approach that makes it possible to achieve maximum maneuverability while avoiding wheel slippage. It develops individual wheel constraints that enable the wheels to be independently controlled while satisfying the desired vehicle motion. Numerical simulation results have shown that this approach can indeed simplify the problem of controlling four steered wheel vehicles.

## I. INTRODUCTION

Because of their high maneuverability characteristics, the interest in vehicles with four steered wheels has been increasing over time. From a series of papers published by the Society of Automotive Engineers [1], [2], [3] and other technical media [4] in the mid-eighties, it seems that the thrust towards these vehicles originated from the automotive industry. The maneuverability problem in robotics was approached by using differential steering systems and omni-wheels for omnidirectional locomotion [5], [6]. Together, these approaches promoted successful development of omnidirectional robots with three steered wheels [6], [7], [8], [9] of negligible slippage. Despite these successes, the problem of controlling robotic vehicles equipped with four steered wheels has not been as successful. This lack of success in

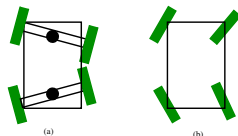


Fig. 1. Typical Wheel Configurations for Four Wheel Steered Vehicles

four steered wheel vehicles may be attributed to the presence of many independently moving points on the vehicle, i.e., the

The authors are with the Department of Mechanical Engineering, North Dakota State University Dept 2490, P.O. Box 6050, Fargo, ND, 58108-6050. Email: majura.selekwa@ndsu.edu, Jonathan.R.Nistler@ndsu.edu

wheels. Therefore, the rigid body kinematic constraints that must be satisfied on such vehicles are generally difficult to meet.

Today, two types of four wheel steered vehicles can be identified as illustrated in Figure 1: vehicles with two sets of mechanically coupled steered wheels (a), and vehicles with independently steered wheels (b). Since the kinematic constraints for vehicles that have mechanically coupled pairs of steered wheels are less stringent, their dynamic models have been easy to develop and control. These models have only two steering angles: one angle for both front wheels and another angle for both rear wheels. One of their characteristic features is the presence of variable relative distances between the wheels and the vehicle's mass center. Many significant results in robotics have been reported based on vehicles with this wheel configuration [10], [11], [12], [13], [14].

Vehicles with independently steered wheels pose a challenge because of the difficulty in satisfying the rigid body kinematic constraints for all wheels in a variety of paths. Many of the proposed alternative approaches alleviate effects of wheel slippage by using circular or square robots [15], [16] and possibly with omnidirectional wheels [17], [18], [19], [20], [21]. Others minimize the wheel slippage by limiting the steering angles to only small values such that the two front wheels can be assumed to have the same steering angle as well as the rear wheels [22], [23].

The key kinematic constraint that must be satisfied by all robotic vehicles is the consistence of the instantaneous center of rotation (ICR) for all wheels and the robot body. Since the location of ICR changes with the path geometry, it is in general to difficult to exploit it. The easiest way of locating the ICR is by constraining it along the perpendicular bisector of the robot's longitudinal centerline. However, this approach limits the vehicle maneuverability, because it automatically dictates the rear wheel angles to mirror the front wheel angles. A closed loop solution for any arbitrary positioning of the ICR has not been fully established. Existing approaches for solving this problem involve some measurements or estimation of the vehicle yaw rate [24], [25], and are related to the early developments on the subject [26], [27]. Since the relationship between the wheel velocities and the vehicle yaw rate is one way causal, with the latter being a result of the former, determining the wheel velocities based on estimated yaw rates may be prone to considerable errors.

This paper develops closed loop constraints for determining the individual wheel steering angles and wheel speeds using the path geometry and the vehicle speed only. These constraints are applied in developing the path tracking con-

troller for the vehicle. The vehicle is assumed to be equipped with appropriate path detection sensors, and odometry. The paper is divided into four sections. Section II formulates wheel constraint equations, and develops a control system for leading the robot along the desired path. Section III presents numerical simulation results, and finally the paper closes with some concluding remarks in Section IV.

## II. VEHICLE MODELING AND CONTROL DESIGN

### A. Kinematic Constraints

The theoretical foundation of the model presented in this section lies in standard methods of analytical dynamics [28], [29], [30], [31], [32]. Figure 2 shows the framework for development of this model. Later on, the vehicle will be assumed to be wholly a non-deformable rigid body such that the relative orientations and positions  $r_{Gi}$ ,  $i = 1, 2, \dots, 4$ , of the wheels from the mass center  $G$  are constant.

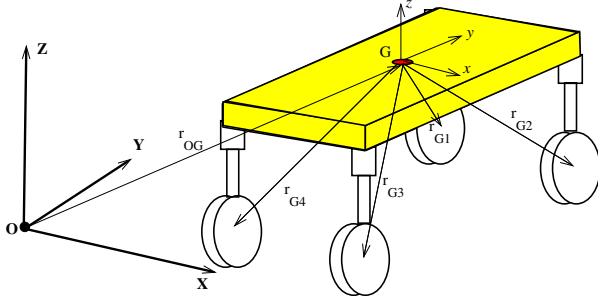


Fig. 2. The configuration the coordinate system for a robotic vehicle

Assume that the frame  $xyz$  is attached to, and moves with the vehicle at its center of mass,  $G$ , such that the  $y$  axis is always pointing in the direction of the vehicle. If the corresponding rotation (Euler) angles of frame  $xyz$  with respect to  $XYZ$  are  $\theta_x$ ,  $\theta_y$ , and  $\theta_z$ , then by using standard coordinate transformation methods [28], [29], [30], the relative position  $(x', y', z')$  of any part of the vehicle can be expressed in the  $XYZ$  frame by using the linear coordinate transformation  $J$  such that

$$\begin{pmatrix} X' \\ Y' \\ Z' \end{pmatrix} = \vec{r}_{OG} + J_G \begin{pmatrix} x' \\ y' \\ z' \end{pmatrix}, \quad (1)$$

where  $\vec{r}_{OG}$  is the relative position of the vehicle's center of mass in the  $XYZ$  inertial frame from its origin, and  $J_G$  is the rotation matrix of the frame  $xyz$  in frame  $XYZ$  about  $G$ . Assuming sequential  $Z-Y-X$  rotations, the matrix  $J_G$  is defined as

$$J_G \triangleq \begin{bmatrix} C_y C_z & C_x S_z + S_x S_y C_z & S_x S_z - C_x S_y C_z \\ -C_y S_z & C_x C_z - S_x S_y S_z & S_x C_z + C_x S_y S_z \\ S_y & -S_x C_y & C_x C_y \end{bmatrix}, \quad (2)$$

with  $C_x \triangleq \cos(\theta_x)$ , and  $S_y \triangleq \sin(\theta_y)$ . Defining  $\vec{r}_{xyz}$  as a point on the vehicle body such that  $\vec{r}_{xyz} \triangleq [x' \ y' \ z']^T$ , then the velocity vector  $\vec{V}$  of this point  $\vec{r}_{xyz}$  on the car as seen from the origin of the  $XYZ$  inertial frame is

$$\vec{V} = \vec{V}_G + \vec{\Omega} \times \vec{r}_{xyz} + J_G \dot{\vec{r}}_{xyz}, \quad (3)$$

where  $\vec{\Omega}$  is the rotational velocity vector of the frame  $xyz$  in frame  $XYZ$  defined as  $\vec{\Omega} \triangleq [\dot{\theta}_x \ \dot{\theta}_y \ \dot{\theta}_z]^T$ , and  $\vec{V}_G \triangleq \dot{\vec{r}}_{OG}$

is the velocity of the mass center. Furthermore, if  $\vec{a}_G \triangleq \ddot{\vec{r}}_{OG}$ , then the acceleration  $\vec{a}$  of the point  $\vec{r}_{xyz}$  also satisfy

$$\vec{a} = \vec{a}_G + \vec{\Omega} \times (\vec{\Omega} \times \vec{r}_{xyz}) + \dot{\vec{\Omega}} \times \vec{r}_{xyz} + 2\vec{\Omega} \times \dot{\vec{r}}_{xyz} + J_G \ddot{\vec{r}}_{xyz} \quad (4)$$

For a ground robotic vehicle with  $n$  wheels, each wheel must move at velocities  $\vec{V}_i$  and accelerations  $\vec{a}_i$  each satisfying (3) and (4) such that the vehicle tracks the desired path  $\vec{r}_{OG}$  at a desired velocity,  $\vec{V}_G$ , and acceleration,  $\vec{a}_G$ , without slippage. Most often, control problems are concerned with satisfying velocity requirements only, with accelerations serving as intermediaries towards achieving the desired velocities.

In the general case where the robotic vehicle runs along a path,  $\vec{p}(X, Y, Z)$ , defined in the inertial frame  $XYZ$ , all three components of each wheel velocity,  $\vec{V}_i$ , must be well coordinated. This is relatively complex endeavor; however, most applications assume that the path,  $\vec{p}(X, Y, Z)$ , is along a flatland such that the  $Z$ -coordinate is constant. Therefore, the control problem reduces to determining only two components of the wheel velocities. Even with this assumption of a flatland path, if  $\vec{r}_{xyz}$  is not constant, then  $\vec{V}_G$  will still have three components, with almost same level of difficulty as that of a 3-D path.

The simplest case of flatland path that has been extensively studied assumes that the vehicle is a rigid body such that  $\dot{\vec{r}}_{xyz} = 0$ , and  $\ddot{\vec{r}}_{xyz} = 0$ . Under this assumption, there exists a single point  $C$  at position  $\vec{r}_{OC}$  in the inertial frame serving as its instantaneous center of zero velocity such that  $\vec{V}_G = \vec{\Omega} \times (\vec{r}_{OC} - \vec{r}_{OG})$ . Therefore, the velocities at the wheel centers can be expressed as

$$\vec{V}_i = \vec{\Omega} \times [\vec{r}_{OC} - (\vec{r}_{OG} + \vec{r}_{Gi})], \quad i = 1, 2, \dots, 4, \quad (5)$$

where  $\vec{r}_{Gi}$  is the position vector of wheel  $i$  from the vehicle's mass center. Again, the problem of controlling the robotic vehicle to track a particular path focuses on determining the wheel velocities,  $\vec{V}_i$ , of (5) such that the robot tracks the desired trajectory,  $\vec{r}_{OG}$ , at the desired velocity,  $\vec{V}_G$ , without wheel slippage. Even for this simplest form of robot navigation control as a rigid body in 2-D path, it is still difficult to coordinate all wheel velocities in a way that the vehicle velocity,  $\vec{V}_G$ , is met.

There are two possible approaches for the vehicle to track the 2-D path  $\vec{p}(X, Y)$ : either track the path of its mass center or track the path of its wheels. A typical configuration of a four steered wheel vehicle tracking a path  $\vec{p}(X, Y)$  on a flat  $XY$  plane is shown in Figure 3. The velocity,  $\vec{V}_i$ , of each wheel can be expressed by the wheel speed,  $V_i$ , and its steering angle,  $\delta_i$ , such that equation (5) is satisfied, with an instantaneous center of zero velocity located at  $C$ .

By tracking the mass center, the wheels can assume any velocities (speeds and steering angles) as long as requirements on  $\vec{r}_G$  and  $\vec{V}_G$  are satisfied. However, this approach can take the wheels into negative obstacles that are close to but not on the tracked path. The second approach, which tracks the path of the wheels, can avoid negative obstacles, but it can also lead the vehicle into positive obstacles that are close

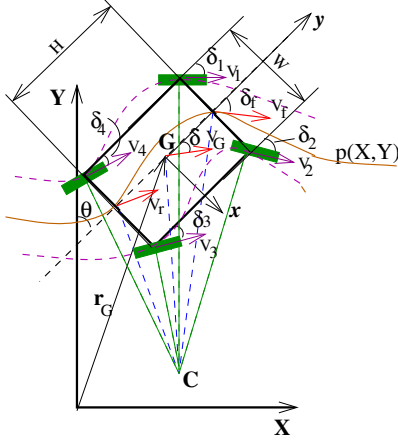


Fig. 3. Typical wheel configuration for a four wheel steered vehicle on a flat surface.

to but not on the wheel path, especially when negotiating corners. We consider the wheel tracking approach only with restrictions that the deviation of G from its path is within acceptable bounds  $\lambda$  such that

$$\|\vec{r}_{OG} - \vec{p}(X, Y)\| \leq \lambda, \quad (6)$$

where  $\|\cdot\|$  is the normal Euclidean norm; therefore the enclosed angles  $\sigma$  at the corners of all allowable traversable paths must satisfy  $\lambda \geq \frac{1}{2}H \tan \frac{1}{2}\sigma$ . For the vehicle in Figure 3, if  $V_f$ ,  $V_G$ , and  $V_r$  respectively are the front, center and rear speeds of the vehicle along the longitudinal centerline with respective directions  $\delta_f$ ,  $\delta_G$  and  $\delta_r$  then kinematic and rigid body constraints on the centerline satisfy  $V_f \cos \delta_f = V_G \cos \delta_G = V_r \cos \delta_r$ , and at the front and rear axles these constraints satisfy  $V_1 \sin \delta_1 = V_f \sin \delta_f = V_2 \sin \delta_2$ , and  $V_3 \sin \delta_3 = V_r \sin \delta_r = V_4 \sin \delta_4$ ; therefore it can be shown that

$$V_f \sin \delta_f - V_r \sin \delta_r = 2(V_G \sin \delta_G - V_r \sin \delta_r) = H\omega, \quad (7)$$

$$V_1 \cos \delta_1 - V_2 \cos \delta_2 = 2(V_f \cos \delta_f - V_2 \cos \delta_2) = W\omega, \quad (8)$$

$$V_4 \cos \delta_4 - V_3 \cos \delta_3 = 2(V_r \cos \delta_r - V_3 \cos \delta_3) = W\omega. \quad (9)$$

where  $\omega$  is the vehicle yaw rate as it negotiates a corner.

Since the only information available to the controller is limited to the path geometry ( $\delta_f$  and  $\delta_r$ ) and the desired robot speed  $V_G$ , the controller is required to establish the values of the wheel speeds  $V_i$ ,  $i = 1, 2, \dots, 4$  and the drive angles  $\delta_i$ ,  $i = 1, 2, \dots, 4$ . In practice, navigation sensors will determine the path direction angle at the front axle,  $\delta_f$ ; however, there will be no corresponding sensors for determining the path direction angle at the rear axle,  $\delta_r$ , for these equations to be determined. If the orientation angle,  $\theta$ , of the vehicle and the path gradient angle  $\rho$  in the inertial frame  $X-Y$  are known where  $\rho = \tan^{-1}(\frac{dY}{dX})$ , then the path direction angles at the front axle  $\delta_f$  and at the rear axle  $\delta_r$  of the vehicle satisfy

$$\delta_f = \frac{\pi}{2} - (\theta + \rho_f); \quad \delta_r = \frac{\pi}{2} - (\theta + \rho_r), \quad (10)$$

where  $\rho_f$  and  $\rho_r$  respectively are the path gradient angles at the front and at the rear axles of the vehicle. A finite path memory function  $M$  is required to monitor the front path gradient angle,  $\rho_f$ , such that at any front axle path coordinates  $(X_f, Y_f)$  and vehicle orientation  $\theta$ ,

$$M(X_f, Y_f) = \rho_f, \quad (11)$$

$$\rho_r = M(X_f - H \sin \theta, Y_f - H \cos \theta). \quad (12)$$

These path gradient angles are used to determine the path orientation parameters in (10). This assumption requires the vehicle to start its motion on a straight line path along the  $Y$  direction for at least distance  $H$  before making turns.

If all angles  $\delta_i$ ,  $i = f, G, r, 1, 2, \dots, 4$  are such that  $|\delta_i| < \frac{\pi}{2}$ , then by combining equations (7)-(9) with the instantaneous center equation (5) leads to the wheel speed constraints<sup>1</sup>

$$V_i = \begin{cases} \frac{V_G \tan \delta_f \csc \delta_i}{\sqrt{1 + \frac{1}{4}(\tan \delta_f + \tan \delta_r)^2}}, & i = 1, 2; \\ \frac{V_G \tan \delta_r \csc \delta_i}{\sqrt{1 + \frac{1}{4}(\tan \delta_f + \tan \delta_r)^2}}, & i = 3, 4; \end{cases} \quad (13)$$

and wheel steer angle constraints

$$\delta_1 = \cot^{-1} \left( \cot \delta_f + \frac{W}{2H} \cot \delta_f [\tan \delta_f - \tan \delta_r] \right), \quad (14)$$

$$\delta_2 = \cot^{-1} \left( \cot \delta_f - \frac{W}{2H} \cot \delta_f [\tan \delta_f - \tan \delta_r] \right), \quad (15)$$

$$\delta_3 = \cot^{-1} \left( \cot \delta_r - \frac{W}{2H} \cot \delta_r [\tan \delta_f - \tan \delta_r] \right), \quad (16)$$

$$\delta_4 = \cot^{-1} \left( \cot \delta_r + \frac{W}{2H} \cot \delta_r [\tan \delta_f - \tan \delta_r] \right), \quad (17)$$

These constraint equations are similar to those of [26], [27], but they are proactive and more explicit requiring information on the vehicle speed  $V_G$  and the path geometry ( $\delta_f, \delta_r$ ) only instead of relying on the vehicle yaw rate  $\omega$ , which essentially is dependent on wheel speeds and angles.

### B. Dynamic Equations

To formulate the dynamic equations for the robot, it is assumed that the wheels will roll without slippage, therefore, the wheel speed  $V_i$  is related to its rotational speed  $\phi_i$  as  $V_i = r_w \phi_i$ , where  $r_w$  is the wheel radius. Figure 4 shows the forces acting on the robot wheel (a) and on the robot body (b). Each wheel is acted on by a total of four forces and three torques: the longitudinal,  $F_{Li}$ , and lateral,  $F_{Ti}$ , ground reactions; the longitudinal,  $R_{Li}$ , and lateral vehicle support reactions,  $R_{Ti}$ ; the steering torque,  $\tau_{Si}$ , the traction torque,  $\tau_{Ti}$ , and the wheel self-aligning torque  $\tau_{Ai}$  (not shown in the figure). The side slip angle for the wheel is  $\gamma_i$ , and the no wheel slippage condition guarantees that  $F_{Li} = R_{Li}$ , and  $F_{Ti} = R_{Ti}$ . The vehicle body is acted by a total of four pairs of wheel reactions:  $R_{Li}$  and  $R_{Ti}$  for  $i = 1, 2, \dots, 4$ .

Assuming that the vehicle weight  $M_{RG}$  is evenly distributed on all wheels, the lateral tire force  $F_{Ti}$  can be approximated as

$$F_{Ti} = \frac{1}{4} M_{RG} \mu(\gamma_i), \quad (18)$$

where  $\mu(\gamma_i)$  is the friction coefficient for a particular side slip angle  $\gamma_i$ ; it can be estimated using either the extended Burckhardt's formula [33]

$$\mu(\gamma_i) = [C_1 - C_1 \exp(-C_2 \gamma_i) - C_3 \gamma_i] \exp(-C_2 \gamma_i V_i), \quad (19)$$

or the Pacejka's formula [34]

$$\mu(\gamma_i) = C_1 \sin \left( C_2 \tan^{-1} \left( C_3 \gamma_i - C_4 (C_3 \gamma_i - \tan^{-1}(C_3 \gamma_i)) \right) \right), \quad (20)$$

<sup>1</sup>Note that  $\lim_{\delta_x, \delta_y \rightarrow 0} [\tan \delta_x \csc \delta_y] = \lim_{\delta_x, \delta_y \rightarrow 0} \left[ \frac{\sin \delta_x}{\sin \delta_y} \sec \delta_x \right] = 1$

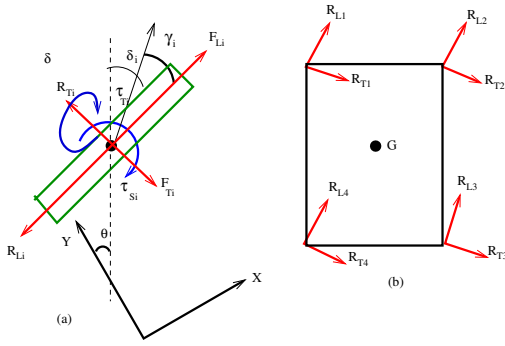


Fig. 4. Forces on Torques acting on wheels and the vehicle body.

where  $C_1, C_2, C_3$ , and  $C_4$  are constants governed by the tire and road contact conditions.

The effects of the wheel self-aligning torque,  $\tau_{Ai}$ , on each wheel can be neglected; therefore, the generalized coordinate vector  $q \in \mathbb{R}^{11}$  for the robotic system will be defined as

$$q = [X_G, Y_G, \theta, \varphi_1, \varphi_2, \varphi_3, \varphi_4, \delta_1, \delta_2, \delta_3, \delta_4]^T, \quad (21)$$

and a corresponding generalized force vector as

$$Q = [F_X, F_Y, \tau_\theta, \tau_{T1}, \tau_{T2}, \tau_{T3}, \tau_{T4}, \tau_{S1}, \tau_{S2}, \tau_{S3}, \tau_{S4}]^T. \quad (22)$$

If the wheel slip angles  $\gamma_i$  are neglected, then the generalized forces  $F_X$  and  $F_Y$  are related to the wheel reactions by

$$F_X = \sum_{i=1}^4 R_{Ti}(\sin \delta_i \cos \theta - \cos \delta_i \sin \theta) + R_{Li} \Psi_i, \quad (23)$$

$$F_Y = \sum_{i=1}^4 R_{Li}(\sin \delta_i \cos \theta - \cos \delta_i \sin \theta) - R_{Ti} \Psi_i, \quad (24)$$

where  $\Psi_i = (\sin \delta_i \sin \theta + \cos \delta_i \cos \theta)$ , and the magnitude of the generalized body torque  $\tau_\theta$  is defined as

$$\tau_\theta = \left| \sum_{i=1}^4 \left[ \vec{r}_{Gi} \times (\vec{R}_{Ti} + \vec{R}_{Li}) \right] \right|. \quad (25)$$

By ignoring the potential energy due to the steering damping and the vehicle suspension system, the corresponding Lagrangian  $\mathcal{L}$  for this system can now be defined as

$$\mathcal{L} = \frac{1}{2} \left[ M_R V_{GX}^2 + M_R V_{GY}^2 + I_R \omega^2 + \sum_{i=1}^4 (I_{wr} \dot{\phi}_i^2 + I_{ws} \dot{\delta}_i^2) \right], \quad (26)$$

where  $M_R$  is the mass of the robot,  $I_R$  its yaw moment of inertia,  $I_{wr}$  the wheel rotational moment of inertia of each wheel about the ground contact, and  $I_{ws}$  is the steering rotational moment of inertia for each wheel. The linear speeds,  $V_{GX}$  and  $V_{GY}$  respectively, are the X- and Y- components of the vehicle velocity  $\vec{V}_G$ , i.e.,

$$V_{GX} = \frac{V_G (\tan \delta_f + \tan \delta_r)}{\sqrt{4 + (\tan \delta_f + \tan \delta_r)^2}}, \quad (27)$$

$$V_{GY} = \frac{2V_G}{\sqrt{4 + (\tan \delta_f + \tan \delta_r)^2}}, \quad (28)$$

By applying the standard Euler-Lagrange equation  $\frac{d}{dt} \left( \frac{\partial \mathcal{L}}{\partial \dot{q}_j} \right) - \frac{\partial \mathcal{L}}{\partial q_j} = Q_j$ ,  $j = 1, 2, \dots, 11$ , the resulting equations of motion can be expressed as

$$\dot{\mathbf{x}} = \mathcal{F}(\mathbf{x}, \mathbf{u}), \quad (29)$$

where the control vector,  $\mathbf{u} \in \mathbb{R}^8$ , comprises of the wheel torques only, i.e.,

$$\mathbf{u} = [\tau_{T1}, \tau_{T2}, \tau_{T3}, \tau_{T4}, \tau_{S1}, \tau_{S2}, \tau_{S3}, \tau_{S4}]^T; \quad (30)$$

the state vector,  $\mathbf{x} \in \mathbb{R}^{14}$ , is defined as

$$\mathbf{x} = [X_G, V_{GX}, Y_G, V_{GY}, \theta, \omega, \delta_1, \beta_1, \delta_2, \beta_2, \delta_3, \beta_3, \delta_4, \beta_4]^T, \quad (31)$$

where  $\beta_i = \dot{\delta}_i$ . The wheel longitudinal forces satisfy

$$R_{Li} = F_{Li} = \frac{1}{r_w} \left( \tau_{Ti} - \frac{I_{wr} \dot{V}_i}{r_w} \right) \quad (32)$$

for each wheel  $i = 1, 2, \dots, 4$ , where  $V_i$ 's are defined as in (13) with  $V_G = \sqrt{V_{GX}^2 + V_{GY}^2}$ , and the lateral forces  $R_{Ti} = F_{Ti}$  are estimated using (18). The  $14 \times 8$  dynamic system (29) can be established by combining the formulations described above.

### C. The Path Tracking Controller

From the model developed in Section II-B, the path tracking control problem is defined as that of finding  $\mathbf{u}$  such that the vehicle runs at the desired speed  $V_{G(ref)}$  and it remains aligned to the path  $\vec{p}(X, Y)$ . Figure 5 shows a simplified structure for this control system.

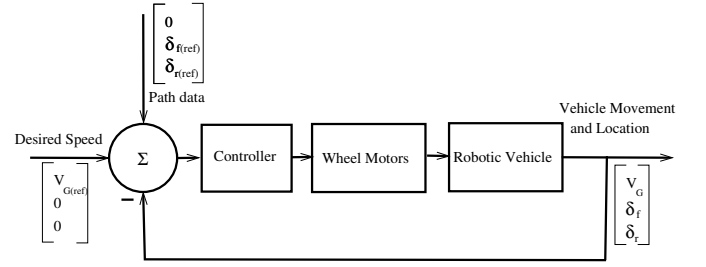


Fig. 5. A simplified layout of the proposed control system.

Many standard multivariable nonlinear control approaches can be applied in developing the required controller for this system. However, the size and structure of this  $14 \times 8$  system will definitely complicate the control design process. The approach used in this paper is to break the control problem into simple individual wheel controllers in a decentralized form. This approach treats the robot as system of objects centered at the vehicle wheels. As such, it assumes that the weight of the vehicle is evenly distributed among the wheels such that application of equation (32) on the wheel yields

$$\left( \frac{M_R}{4} + m_w \right) \dot{V}_i = \frac{1}{r_w} \left( \tau_{Ti} - \frac{I_{wr} \dot{V}_i}{r_w} \right), \quad (33)$$

where  $m_w$  is the mass of the wheel. This, along with the corresponding steering equations for each wheel, neglecting the steering wheel friction, leads to

$$\begin{bmatrix} \dot{V}_i \\ \dot{\delta}_i \\ \dot{\beta}_i \end{bmatrix} = \begin{bmatrix} \frac{4r_w \tau_{Ti}}{M_R r_w^2 + 4(I_{wr} + m_w r_w^2)} \\ \beta_i \\ \frac{\tau_{Si}}{I_{ws}} \end{bmatrix}. \quad (34)$$

Now, it is required to find  $\tau_{Ti}$  and  $\tau_{Si}$  such that the wheel motion satisfies the references,  $V_{i(ref)}$  and  $\delta_{i(ref)}$ , compatible

with  $[V_{G(ref)}, \delta_{f(ref)}, \delta_{r(ref)}]^T$ . At this point, only a simple decoupled proportional controller has been numerically simulated under discrete time domain as

$$\begin{bmatrix} \tau_{Ti}(k+1) \\ \tau_{Si}(k+1) \end{bmatrix} = \begin{bmatrix} {}^P K_T [V_{i(ref)} - V_i(k)] \\ {}^P K_S [\delta_{i(ref)} - \delta_i(k)] \end{bmatrix}, \quad (35)$$

where  ${}^P K_T$  and  ${}^P K_S$  are the traction, and steering proportional control gains. This controller is not only simple, but also it is less dependant of the model accuracy; additionally, the controller uses easily measurable inputs, i.e., the desired vehicle speed and the path geometry.

### III. SIMULATION RESULTS

The proposed controller was numerically simulated on a robotic vehicle whose physical data is shown in Table I.

TABLE I  
SIMULATION VEHICLE PHYSICAL PARAMETERS

Quantity	Value	Units	Quantity	Value	Units
$M_R$	50.00	$Kg$	$m_w$	3.5	$Kg$
$I_R$	5.50	$Kgm^2$	$r_w$	0.085	$m$
$H$	1.00	$m$	$I_{ws}$	0.009	$Kgm^2$
$W$	0.75	$m$	$I_{wr}$	0.025	$Kgm^2$

Figures 6 through 8 show some of the simulation results obtained along a path illustrated in Figure 6 at a speed of  $V_G = 1 \text{ m/s}$ . The theoretical values of the wheel speeds and

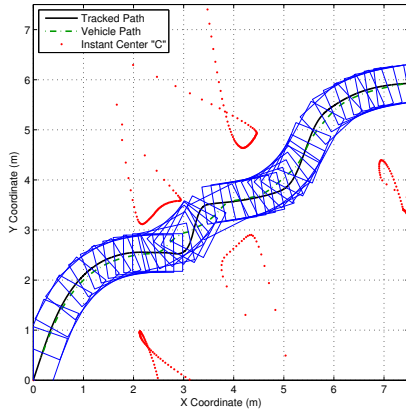


Fig. 6. The simulated robot trajectory

steering angles were computed in two approaches; the first approach used the path gradient to determine the instantaneous centers shown in red dots, then the speeds of the wheels and their directions were determined geometrically using these instantaneous centers. The second approach, also used the path gradient to determine the angles  $\delta_r$  and  $\delta_f$ ; these angles were used in equations (13) through (17). Both approaches yielded identical results.

The proposed decoupled controller (35) was simulated on the vehicle described above at a sampling interval of  $1 \text{ ms}$ ; the controller gains were set at  ${}^P K_T = 120$  and  ${}^P K_S = 230$ . The vehicle speed was assumed to remain constant at  $1.0 \text{ m/s}$ , and the front axle path angle,  $\delta_f$ , was estimated by using the path gradient at the front axle, while the rear

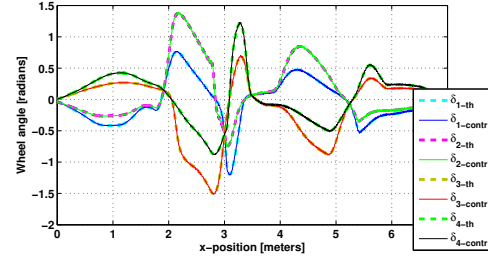


Fig. 7. Controlled compared to computed wheel angles

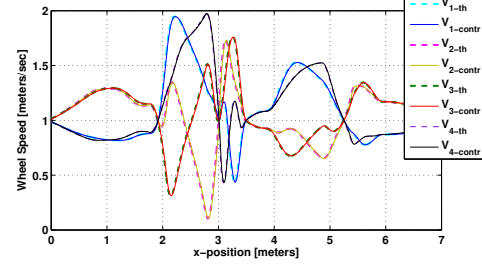


Fig. 8. Controlled compared to computed wheel speeds

axle path angle,  $\delta_r$ , was determined by using the memory function (11)-(12). Figures 7 and 8 respectively show the results obtained on the wheel angles and wheel speeds as compared to the predicted values. Because of the exact similarity between the controlled values and the theoretical values, it appears in these Figures as if each wheel is represented by one curve only, instead of two: the controlled and the theoretical. The controlled values for each wheel have a 'contr' subscript while the theoretical values have a subscript 'th'. This similarity is an indication that this simple controller generated wheel speeds and angles that drive the robot along the path as perfectly as predicted by the theory.

The control torques for the simulated vehicle are shown in Figures 9 and 10. The magnitudes of the traction torques increased whenever the corresponding wheel speeds changed rapidly, and remained almost zero when the wheel speed was held at near constant values. The steering torques showed to be very actively busy throughout the simulation interval, especially when negotiation corners. Both the steering torques and the traction torques were within  $\pm 15 \text{ Nm}$  for the simulated vehicle, which is a reasonable value.

### IV. SUMMARY AND CONCLUSIONS

This paper has presented eight explicit kinematic constraint equations that must be satisfied by four wheel steered vehicles. These constraints depend on the desired vehicle speed and the path geometry. Generally, the resulting vehicle model is relatively large, i.e., fourteenth order; however, by decentralizing the control system, it is possible to control the vehicle using four simple controllers at each wheel. Simulation results have demonstrated this concept that. Since certain speeds and angle demands may call for excessively high torques, it is important to limit the maximum allowable vehicle speed  $V_G$  at any given corner angle  $\sigma$ . The next phase of the research will focus on implementing the proposed

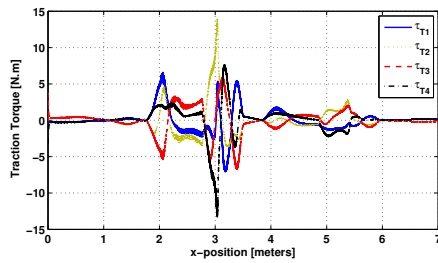


Fig. 9. Simulated Traction Torques

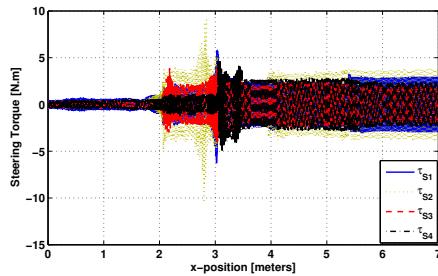


Fig. 10. Simulated Steering Torques

control approach on an experimental 4WS/4WD robotic vehicle and compare its performance to those that assume the axle wheels to have the same steering angles, and those that estimate the vehicle yaw rate.

#### REFERENCES

- [1] S. Sano, Y. Furukawa, and S. Shiraishi, "Four wheel steering system with rear wheel steer angle controlled as a function of steering wheel angle," *SAE Paper No. 860625*, 1986.
- [2] T. Takiguchi, N. Yasuda, S. Furutani, H. Kanazawa, and H. Inoue, "Improvement of vehicle dynamics by vehicle-speed-sensing four-wheel steering system," *SAE Paper No. 860624*, 1986.
- [3] J. C. Whitehead, "Four wheel steering: Maneuverability and high speed stabilization," *SAE Paper No. 880642*, 1988.
- [4] Y. Furukawa, N. Yuhara, S. Sano, H. Takeda, and Y. Matsushita, "A review of four-wheel steering studies from the viewpoint of vehicle dynamics and control," *Vehicle System Dynamics*, vol. 18, no. 1–3, pp. 151–186, 1989.
- [5] J. Agull, S. Cardona, and J. Vivancos, "Dynamics of vehicles with directionally sliding wheels," *Mechanism and Machine Theory*, vol. 24, no. 1, pp. 53 – 60, 1989.
- [6] R. Balakrishna and A. Ghosal, "Modeling of slip for wheeled mobile robots," *Robotics and Automation, IEEE Transactions on*, vol. 11, no. 1, pp. 126 –132, Feb. 1995.
- [7] G. Campion, G. Bastin, and B. D'Andrea-Novell, "Structural properties and classification of kinematic and dynamic models of wheeled mobile robots," in *Robotics and Automation, 1993. Proceedings., 1993 IEEE International Conference on*, May 1993, pp. 462 –469 vol.1.
- [8] K. Kanjanawanishkul and A. Zell, "Path following for an omnidirectional mobile robot based on model predictive control," in *Robotics and Automation, 2009. ICRA '09. IEEE International Conference on*, May 2009, pp. 3341 –3346.
- [9] J. Vazquez and M. Velasco-Villa, "Computed-torque control of an omnidirectional mobile robot," in *Proc. 4th Int. Conf. on Electrical and Electronics Engg. - ICEEE 2007*, Sept. 2007, pp. 274 –277.
- [10] N. Matsumoto and M. Tomizuka, "Vehicle lateral velocity and yaw rate control with two independent control inputs," in *American Control Conference, 1990*, May 1990, pp. 1868 –1875.
- [11] J. Ackermann and W. Sienel, "Robust yaw damping of cars with front and rear wheel steering," *Control Systems Technology, IEEE Transactions on*, vol. 1, no. 1, pp. 15 –20, Mar. 1993.
- [12] J. Borenstein, "Control and kinematic design of multi-degree-of freedom mobile robots with compliant linkage," *Robotics and Automation, IEEE Transactions on*, vol. 11, no. 1, pp. 21 –35, Feb. 1995.
- [13] X. Gao, B. McVey, and R. Tokar, "Robust controller design of four wheel steering systems using  $\mu$  synthesis techniques," in *Decision and Control, 1995., Proceedings of the 34th IEEE Conference on*, vol. 1, Dec. 1995, pp. 875 –882 vol.1.
- [14] M. A. Vilaplana, O. Mason, D. J. Leith, and W. E. Leithead, "Control of yaw rate and sideslip in 4-wheel steering cars with actuator constraints," in *Switching and Learning in Feedback Systems*, ser. Lecture Notes in Computer Science, R. Murray-Smith and R. Shorten, Eds. Springer Berlin / Heidelberg, 2005, vol. 3355, pp. 201–222.
- [15] M. Wada, "Virtual link model for redundantly actuated holonomic omnidirectional mobile robots," in *Proc. of 2006 IEEE Int. Conf. on Robotics and Automation (ICRA 2006)*, May 2006, pp. 3201 –3207.
- [16] M. Lauria, I. Nadeau, P. Lepage, Y. Morin, P. Giguere, F. Gagnon, D. Letourneau, and F. Michaud, "Design and control of a four steered wheeled mobile robot," in *Proc. 32nd Annual Conference on IEEE Industrial Electronics (IECON 2006)*, Nov. 2006, pp. 4020 –4025.
- [17] P. Muir and C. Neuman, "Kinematic modeling for feedback control of an omnidirectional wheeled mobile robot," in *Robotics and Automation. Proceedings. 1987 IEEE International Conference on*, vol. 4, Mar. 1987, pp. 1772 – 1778.
- [18] K.-S. Byun, S.-J. Kim, and J.-B. Song, "Design of a four-wheeled omnidirectional mobile robot with variable wheel arrangement mechanism," in *Proc. 2002 IEEE International Conference on Robotics and Automation (ICRA '02)*, vol. 1, May 2002, pp. 720 – 725 vol.1.
- [19] C. Leng and Q. Cao, "Velocity analysis of omnidirectional mobile robot and system implementation," in *Proc. 2006 IEEE International Conference on Automation Science and Engineering (CASE '06)*, Oct. 2006, pp. 81 –86.
- [20] C.-C. Tsai, Z.-R. Wu, Z.-C. Wang, and M.-F. Hisu, "Adaptive dynamic motion controller design for a four-wheeled omnidirectional mobile robot," in *Proc. 2010 Int. Conference on System Science and Engineering (ICSSE)*, July 2010, pp. 233 –238.
- [21] O. Purwin and R. D'Andrea, "Trajectory generation and control for four wheeled omnidirectional vehicles," *Robotics and Autonomous Systems*, vol. 54, no. 1, pp. 13 – 22, 2006.
- [22] W. Langson and A. Alleyne, "Multivariable bilinear vehicle control using steering and individual wheel torques," in *Proc of the 1997 American Control Conference.*, vol. 2, Jun 1997, pp. 1136 –1140.
- [23] Y. Yavin, "Modelling the motion of a car with four steerable wheels," *Mathematical and Computer Modelling*, vol. 38, no. 10, pp. 1029 – 1036, 2003.
- [24] C. Connette, C. Parlitz, M. Hagele, and A. Verl, "Singularity avoidance for over-actuated, pseudo-omnidirectional, wheeled mobile robots," in *Proc. 2009 IEEE International Conference on Robotics and Automation -ICRA '09.*, May 2009, pp. 4124 –4130.
- [25] M. Makatchev, J. J. McPhee, S. K. Tso, and S. Y. T. Lang, "System design, modelling, and control of a four-wheel-steering mobile robot," in *Proc. 19th Chinese Control Conference*, 2000, pp. 759–763.
- [26] H. Itoh and A. Oida, "Dynamic analysis of turning performance of 4wd-4ws tractor on paved road," *Journal of Terramechanics*, vol. 27, no. 2, pp. 125 – 143, 1990.
- [27] H. Itoh, A. Oida, and M. Yamazaki, "Numerical simulation of a 4wd-4ws tractor turning in a rice field," *Journal of Terramechanics*, vol. 36, no. 2, pp. 91 – 115, 1999.
- [28] P. Muir and C. P. Neuman, "Kinematic modeling of wheeled mobile robots," Robotics Institute, Pittsburgh, PA, Tech. Rep. CMU-RI-TR-86-12, June 1986.
- [29] H. Baruh, *Analytical Dynamics*. McGraw-Hill International, 1998.
- [30] M. Tarokh, L. Mireles, and G. McDermott, "Two approaches to kinematics modelling of articulated rovers," Department of Computer Science, San Diego State University, Report CSSR-02, October 2005.
- [31] A. Betourne and G. Campion, "Dynamic modelling and control design of a class of omnidirectional mobile robots," in *Proc. 1996 IEEE Int. Conf. on Robotics and Automation.*, vol. 3, Apr 1996, pp. 2810 –2815.
- [32] J. Alexander and J. Maddocks, "On the Kinematics of Wheeled Mobile Robots," *The International Journal of Robotics Research*, vol. 8, no. 5, pp. 15–27, 1989.
- [33] M. Burckhardt and J. Reimpell, *Fahrwerktechnik: Radschlupf-Regelsysteme*. Germany: Vogel-Verlag, 1993.
- [34] H. Pacejka and E. Bakker, "The magic formula tyre model," in *Proc. 1st Int. colloq. on tyre models for vehicle dynamics analysis*, 1991, pp. 1–18.